

Statistical computation of Boltzmann entropy and estimation of the optimal probability density function from statistical sample

Ning Sui¹, Min Li² and Ping He^{1,3,4*}

¹College of Physics, Jilin University, Changchun 130012, China

²Changchun Artificial Satellite Observatory, Chinese Academy of Sciences, Changchun 130117, China

³Center for High Energy Physics, Peking University, Beijing 100871, China

⁴State Key Laboratory of Theoretical Physics, Institute of Theoretical Physics, Chinese Academy of Sciences, Beijing 100190, China

7 September 2021

ABSTRACT

In this work, we investigate the statistical computation of the Boltzmann entropy of statistical samples. For this purpose, we use both histogram and kernel function to estimate the probability density function of statistical samples. We find that, due to coarse-graining, the entropy is a monotonic increasing function of the bin width for histogram or bandwidth for kernel estimation, which seems to be difficult to select an optimal bin width/bandwidth for computing the entropy. Fortunately, we notice that there exists a minimum of the first derivative of entropy for both histogram and kernel estimation, and this minimum point of the first derivative asymptotically points to the optimal bin width or bandwidth. We have verified these findings by large amounts of numerical experiments. Hence, we suggest that the minimum of the first derivative of entropy be used as a selector for the optimal bin width or bandwidth of density estimation. Moreover, the optimal bandwidth selected by the minimum of the first derivative of entropy is purely data-based, independent of the unknown underlying probability density distribution, which is obviously superior to the existing estimators. Our results are not restricted to one-dimensional, but can also be extended to multivariate cases. It should be emphasized, however, that we do not provide a robust mathematical proof of these findings, and we leave these issues with those who are interested in them.

Key words: methods: data analysis – methods: numerical – methods: statistical – cosmology: theory – large-scale structure of Universe.

1 INTRODUCTION

Entropy is very important in thermodynamics and statistical mechanics. In fact, it is the key concept, upon which the equilibrium statistical mechanics is formulated (Landau & Lifshitz 1996; Huang 1987), and from which all the other thermodynamical quantities can be derived. Also, the increasing of entropy shows the time-evolutionary direction of a thermodynamical system. The concept of entropy can even be applied to non-thermodynamical systems such as information theory, in which entropy is a measure of the uncertainty in a random variable (Shannon 1948; Shunsuke 1993), and to non-ordinary thermodynamical systems such as self-gravitating systems, in which the dominating microscopic interaction between particles is long-ranged (Lynden-Bell 1967; Campa et al. 2009). The latter is relevant to our studies, in which we formulated a framework of equilibrium statistical mechanics for self-gravitating systems (He & Kang 2010, 2011;

Kang & He 2011; He 2012a,b). In these works, we demonstrated that the Boltzmann entropy

$$S_B[F] = - \int F(\mathbf{v}) \ln F(\mathbf{v}) d^3\mathbf{v} \quad (1)$$

is also valid for self-gravitating systems, in which $F(\mathbf{v})$ is the system's probability density function (PDF, hereafter).

Hence, the PDF is necessary for computing the systems' entropy, but often, instead of giving an analytic form of PDF, we have to deal with a thermodynamical system that is in data-form. For instance, Helmi & White (1999) performed numerical simulations to study satellite galaxy disruption in a potential resembling that of the Milky Way. In their work, the coarse-grained Boltzmann entropy is used as a measure of the phase-mixing to indicate how mixing of disrupted satellites can be quantified. The analytic PDF is unavailable, and hence they derived the coarse-grained PDF from the simulation data by histogram, that is, by taking a partition in the 6D phase-space and counting how many particles fall in each 6D cell.

So, with analytic PDF unavailable, it is indispensable to compute the system's entropy from the data-based samples. This seemingly easy computation, however, is plagued with some unexpected

* E-mail: hep@itp.ac.cn

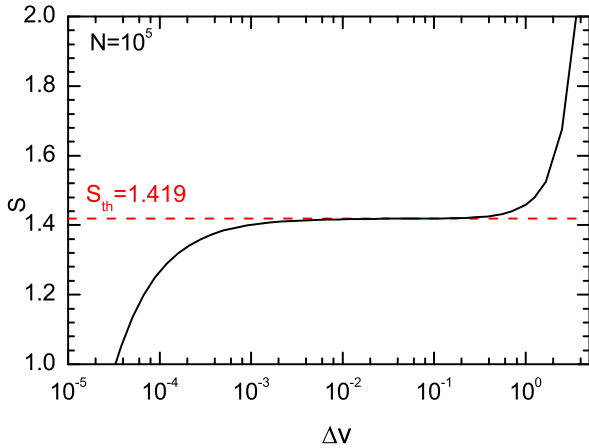


Figure 1. Illustration of the monotonic behaviour of $S(\Delta v)$. The underlying distribution is the univariate standard normal distribution, from which the data set is randomly drawn, with the sample size $N = 10^5$. Δv is the bin width of the one-dimensional histogram, and S is evaluated by equation (1), but with $\hat{F}_{\Delta v}(v)$ instead of $F(v)$. $S(h)$, computed by kernel estimation, exhibits the similar behaviour with respect to the bandwidth h . S_{th} , shown with the dashed line, is directly computed by using the analytical univariate standard normal PDF of equation (4).

troubles. As we have seen in equation (1), the evaluation of entropy is actually related to the estimation of probability density, which is one of the most important techniques in exploratory data analysis (EDA). Usually, $\hat{F}_{\Delta v}(v)$, the estimation of the underlying unknown PDF $F(\mathbf{v})$ of a statistical sample, is derived by data binning, i.e. histogram (Gentle 2009), just as Helmi & White (1999). However, in the real practice, we find the following interesting phenomenon. See Figure 1, the resulting entropy S depends on the bin width Δv , monotonically increasing with the bin width, and thus it is troublesome to select an appropriate bin width of histogram for computing the entropy.

Prior to our study, there have been many investigations on how to make the optimal probability density estimation of statistical samples (Scott 1992; Gentle 2009). Histogram is the mostly used method, in which the bin width is its characteristic parameter. A larger bin width produces over-smooth estimation and the PDF looks smoother and featureless, while a smaller bin width produces under-smooth estimation so that the resulting PDF has large fluctuations and spurious bumps. Hence, the selection of an optimal bin width is indeed an important task in EDA, and such an effort can be dated back to Sturges (1926), but the famous selector for optimal bin width is given by Scott (1979). Usually, the optimal bin width is obtained by minimizing the asymptotic mean integrated squared error (AMISE), which is a tradeoff between the squared bias and variance. Contrary to the conventional treatment, however, Knuth (2013) proposed a straightforward data-based method of determining the optimal number of bins in a uniform bin-width histogram using Bayesian probability theory.

Another commonly used density estimation method is kernel estimation method, which was first introduced by Parzen (1962) and Rosenblatt (1956) and is considered to be much superior to the histogram method (Jones et al. 1996). With kernel density estimation, we arrive at the similar results as with histogram that the entropy increases as a monotonic function of the kernel bandwidth h .

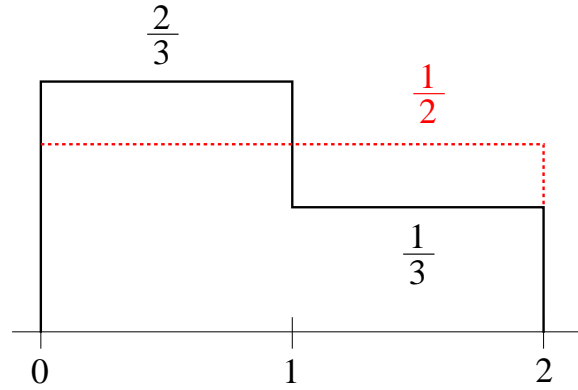


Figure 2. The origin of the monotonicity of $S(\Delta v)$ versus Δv is caused by coarse-graining of the PDF. The step solid line and the dotted line indicate the fine-grained and coarse-grained PDF, respectively. The entropy evaluated with coarse-grained PDF is larger than that with fine-grained PDF. See Section 2.1 for detail. This explanation is also applicable to $S(h)$ versus h .

Besides the two main methods, there are also other methods of density estimation, such as average shifted histogram, orthogonal series estimators (Gentle 2009; Scott 1992, 2004). We just focus on histogram and kernel methods in this work.

Investigations on histogram and kernel estimation have indeed provided us with useful criteria for optimal bin width of histogram or bandwidth of kernel function (Silverman 1986; Jones et al. 1996; Wand 1997), yet all these criteria need to take into account the functional form of the true PDF, which is usually unavailable. So it is a difficulty on how to select an optimal bin width or bandwidth for computing the entropy. Fortunately, by large amounts of numerical experiments, we find that the first derivatives of $S(\Delta v)$ with respect to Δv for histogram estimation, or of $S(h)$ with respect to h for kernel estimation, correspond to the optimal bin width and bandwidth in all the cases we considered in this work.

In this paper, we describe our numerical experiments and demonstrate this finding in detail. Although we do not provide a robust mathematical proof of this finding, we suggest that the first derivative of entropy be regarded as an alternative selector other than the usual AMISE to pick out an optimal bin width of histogram and bandwidth of kernel estimation. The paper is organized as follows. In Section 2, we introduce our methods and describe the working procedure. In Section 3, we present the results. Finally, we give our conclusions and discussions in Section 4.

2 METHODS AND PROCEDURE

2.1 Origin of the monotonicity of $S(\Delta v)$ and $S(h)$

We demonstrate the origin of the monotonicity of $S(\Delta v)$ versus Δv . See Figure 2, we design a simple one-dimensional normalized experimental PDF, as:

$$f_1(v) = \begin{cases} \frac{2}{3}, & 0 < v < 1, \\ \frac{1}{3}, & 1 < v < 2, \\ 0, & \text{otherwise,} \end{cases} \quad (2)$$

with which the entropy evaluated by equation (1) is $S_1 = \ln 3 - \frac{2}{3} \ln 2$. Next, the averaged, or coarse-grained, PDF within the inter-

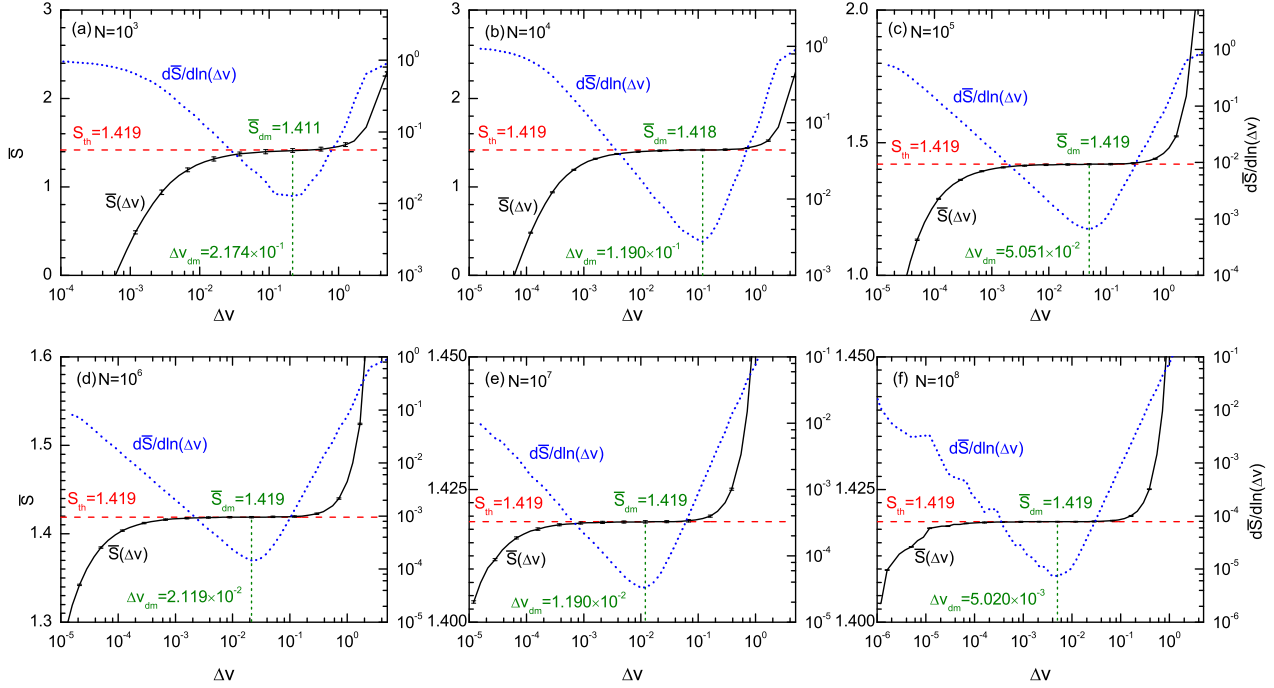


Figure 3. $\bar{S}(\Delta v)$, the averaged entropy evaluated by histogram density estimation and its first derivative w.r.t to Δv , $d\bar{S}/d\ln(\Delta v)$, for the one-dimensional standard normal distribution of equation (4). Error bars of $\bar{S}(\Delta v)$ curves indicate the standard deviation. In every case, the mean and the standard deviation are evaluated with 50 instances. Δv is the bin width of the histogram. In every panel, the left vertical axis on the left represents the entropy S , and the right vertical axis represents the first derivative, $d\bar{S}/d\ln(\Delta v)$. The entropies and their derivatives as functions of Δv are indicated as solid and dotted lines, respectively. For the visual clarity, the derivatives are exhibited in logarithmic scale. The subscript ‘dm’ in the figure indicates ‘derivative’s minimum’, with $\bar{S}_{dm} \equiv S(\Delta v_{dm})$. S_{th} , shown with dashed lines, is the entropy evaluated with analytical PDF of equation (4).

val $0 < v < 2$ can be easily derived and normalized as:

$$f_2(v) = \begin{cases} \frac{1}{2}, & 0 < v < 2, \\ 0, & \text{otherwise.} \end{cases} \quad (3)$$

So, the entropy evaluated with this coarse-grained PDF f_2 is, $S_2 = \ln 2$, and we can immediately see that $S_2 > S_1$. Hence, the monotonicity of $S(\Delta v)$ versus Δv is caused by the coarse-graining of PDF. The same explanation is also applicable to the monotonicity of $S(h)$ versus h .

Beyond the monotonicity of $S(\Delta v)$, however, there should be another important feature hiding in the $S(\Delta v)$ curve. By scrutinizing $S(\Delta v)$ of Figure 1, we speculate that the first derivative of $S(\Delta v)$ with respect to Δv , might take its local minimum around the cross point of S_{th} and $S(\Delta v)$. If this is the case, then we can use this property to construct a selector of optimal bin width of histogram, so that we can compute the entropy to the best extent. We will verify this speculation below.

2.2 Three experimental PDFs

Our strategy is briefly described as follows. First, choose some analytical PDFs, and with Monte Carlo technique, we draw N random data from these analytical PDFs. With these statistical samples, we can construct the estimators $\hat{F}_{\Delta v}(v)$ or $\hat{F}_h(v)$ of the true PDFs, depending on whether using histogram or kernel estimation. Secondly, we can compute the entropy by equation (1), with $\hat{F}_{\Delta v}(v)$ or $\hat{F}_h(v)$ replacing the true PDFs. In this way, we derive the curves of $S(\Delta v)$ or $S(h)$.

Meanwhile, the entropy can be exactly evaluated with these analytical PDFs, denoted as S_{th} . These exact results can be used to calibrate our empirical results of $S(\Delta v)$ or $S(h)$, and to help select the optimal bin width or bandwidth.

For this purpose, we choose three analytical PDFs for the experiments. The first is the one-dimensional standard normal distribution:

$$F(v) = \frac{1}{\sqrt{2\pi}} e^{-\frac{v^2}{2}}, \quad -\infty < v < \infty, \quad (4)$$

whose $S_{th} = 1.419$.

The second experimental PDF is the one-dimensional power-law function:

$$F(v) = 1 - \frac{16}{9}v^2, \quad -\frac{3}{4} < v < \frac{3}{4}, \quad (5)$$

whose $S_{th} = 0.2804$. Unlike the first one, this power-law distribution is non-extended for its random variable v .

The third one is the three-dimensional isotropic standard normal distribution PDF:

$$F(\mathbf{v}) = \frac{1}{(2\pi)^{3/2}} e^{-\frac{\mathbf{v}^2}{2}}, \quad -\infty < \mathbf{v} < \infty, \quad (6)$$

in which $\mathbf{v} \equiv (v_1, v_2, v_3)$ and $S_{th} = 4.257$. This PDF can be further reduced to a one-dimensional distribution, whose PDF is:

$$F(v) = \sqrt{\frac{2}{\pi}} v^2 e^{-\frac{v^2}{2}}, \quad 0 < v < \infty. \quad (7)$$

This reduced one-dimensional distribution, unlike the previous two distributions, is asymmetric in the random variable v .

Table 1. Results derived from histogram estimation. Listed are the mean \bar{S}_{dm} and the variance $\sigma(\bar{S}_{\text{dm}})$ of the entropy at the minimum point, Δv_{dm} , of the derivative of entropy for the three experimental PDFs addressed in Section 2.2. The mean and the variance are evaluated from 50 instances with different sets of random numbers. Sample sizes for the experiments range from 10^3 to 10^8 . To compare with, the theoretical results S_{th} for the three distributions are 1.419, 0.284, and 4.257, respectively.

N	1D normal			1D power-law			3D normal		
	Δv_{dm}	\bar{S}_{dm}	$\sigma(\bar{S}_{\text{dm}})$	Δv_{dm}	\bar{S}_{dm}	$\sigma(\bar{S}_{\text{dm}})$	Δv_{dm}	\bar{S}_{dm}	$\sigma(\bar{S}_{\text{dm}})$
10^3	2.174×10^{-1}	1.411	2.099×10^{-2}	6.250×10^{-2}	0.2756	9.919×10^{-3}	1.170×10^{-1}	4.226	4.003×10^{-2}
10^4	1.190×10^{-1}	1.418	6.643×10^{-3}	2.419×10^{-2}	0.2790	3.121×10^{-3}	6.511×10^{-2}	4.254	1.083×10^{-2}
10^5	5.051×10^{-2}	1.419	2.115×10^{-3}	8.721×10^{-3}	0.2797	4.941×10^{-4}	3.669×10^{-2}	4.256	3.697×10^{-3}
10^6	2.119×10^{-2}	1.419	8.134×10^{-4}	3.178×10^{-3}	0.2812	2.464×10^{-5}	1.546×10^{-2}	4.256	1.295×10^{-3}
10^7	1.190×10^{-2}	1.419	2.045×10^{-4}	1.786×10^{-3}	0.2805	1.326×10^{-5}	8.695×10^{-3}	4.257	4.184×10^{-4}
10^8	5.020×10^{-3}	1.419	8.081×10^{-5}	1.004×10^{-3}	0.2804	6.098×10^{-7}	1.151×10^{-3}	4.257	1.049×10^{-4}
theoretic	–	1.419	–	–	0.2804	–	–	4.257	–

These S_{th} of the three cases are explicitly indicated in the figures and tables below.

3 RESULTS

3.1 Histogram estimation

As described above, PDF of statistical samples can be estimated mainly by histogram and kernel methods. We first present the results by histogram estimation. Figure 3 shows the experiments with the one-dimensional standard normal distribution of equation (4). We do the experiments of the sample size N ranging from 10^3 to 10^8 , and in every case, we compute $S(\Delta v)$ with different sets of random numbers to give, say 50, instances. With these 50 instances, we can derive both the mean \bar{S} and the variance σ of the entropy as a function of Δv . These results are shown in panels from (a) to (f), respectively, and we can see that the variances of all cases are very small. The first derivative of $\bar{S}(\Delta v)$ with respect to Δv , $d\bar{S}(\Delta v)/d\ln(\Delta v)$, is also numerically evaluated and shown in the corresponding panels. From this figure, we find that: (1) in all cases, the derivative has a minimum around the cross point of the curve $\bar{S}(\Delta v)$ and the straight line S_{th} , (2) the minimum of the derivative goes to zero with increasing sample size N , and (3) Δv_{dm} , at which the derivative takes its minimum, approaches the abscissa of the cross point of $\bar{S}(\Delta v)$ and S_{th} , such that $\bar{S}(\Delta v_{\text{dm}})$ asymptotically approaches S_{th} .

With exactly the same procedures, we do experiments with another two analytical PDFs, i.e. the one-dimensional power-law and three-dimensional isotropic standard normal distribution, of equations (5) and (6), respectively. The above findings are also applied to these two cases. In Table 1, we give the relevant means and variances at Δv_{dm} for all the cases above mentioned.

Note that in Figure 3, we show the first derivative in the form of $d\bar{S}/d\ln(\Delta v)$, rather than $d\bar{S}/d\Delta v$. We can see from the figure, that at Δv_{dm} , $\bar{S}(\Delta v)$ are nearly flat, that is, $d\bar{S}/d\Delta v \sim 0$. Hence,

$$\begin{aligned} \left. \frac{d^2 \bar{S}}{d(\ln \Delta v)^2} \right|_{\Delta v_{\text{dm}}} &= \Delta v \left. \frac{d\bar{S}}{d(\Delta v)} \right|_{\Delta v_{\text{dm}}} + \Delta v^2 \left. \frac{d^2 \bar{S}}{d(\Delta v)^2} \right|_{\Delta v_{\text{dm}}} \\ &\approx \Delta v^2 \left. \frac{d^2 \bar{S}}{d(\Delta v)^2} \right|_{\Delta v_{\text{dm}}} = 0. \end{aligned}$$

So the minima of $d\bar{S}/d\ln(\Delta v)$ and $d\bar{S}/d\Delta v$ are nearly at the same places.

3.2 Kernel estimation

A non-negative real-valued function $K(u)$ is called a kernel function, if satisfying the following two conditions:

$$\int_{-\infty}^{+\infty} K(u) du = 1; \quad K(u) = K(-u).$$

The PDF of a statistical sample, x_i , with i running from 1 to the sample size N , can be estimated by using the kernel function:

$$\hat{F}_h(x) = \frac{1}{hN} \sum_{i=1}^N K\left(\frac{x-x_i}{h}\right), \quad (8)$$

in which h is the bandwidth of the kernel. If the kernel is a derivable function, then $\hat{F}_h(x)$ is also derivable. For this reason, kernel estimation is believed to be superior to histogram method.

The kernel function we used here is Epanechnikov (1969) function $K_e(u)$:

$$K_e(u) = \frac{3}{4}(1-u^2), \quad -1 < u < 1, \quad (9)$$

who has the highest efficiency, in contrast to other kernel functions, to yield the optimal rate of convergence of the mean integrated squared error (Silverman 1986; Gentle 2009).

We give the results from kernel estimation for one-dimensional normal distribution in Figure 4 and the relevant means and variances for all cases at Δv_{dm} in Table 2. These results are all parallel to the previous results from histograms. Again, we can see that the minimum of the first derivative of $S(h)$ can be regarded as a selector for the optimal bandwidth h_{dm} . Compared with the histogram estimation, the advantages of kernel estimation are obvious, in that all the curves, $S(h)$ and dS/dh are smooth and should be derivable.

We also considered other kernel functions, such as uniform and Gaussian (Silverman 1986). The results are the same as with Epanechnikov (not shown).

3.3 Comparison with previous estimators

Prior to our results, there are some well-known estimators for the optimal bin width of histogram or bandwidth of kernel estimation. The Scott (1979) optimal bin width is one of them,

$$\Delta v^* = \left[\frac{6}{R(f')} \right]^{1/3} N^{-1/3}, \quad (10)$$

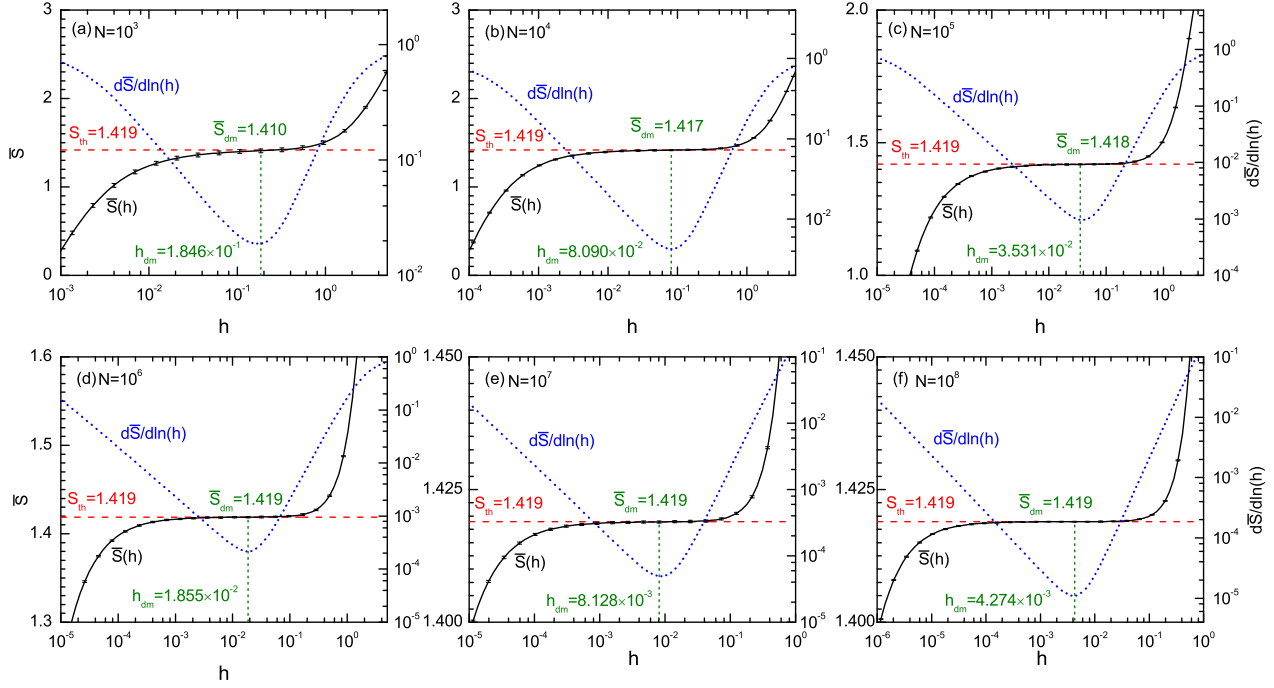


Figure 4. $\bar{S}(h)$, the averaged entropy evaluated with kernel estimation and its first derivative w.r.t to h , $d\bar{S}/d\ln(h)$, for the one-dimensional standard normal distribution of equation (4). The kernel function is the Epanechnikov (1969) form, and h is the bandwidth of the kernel function. Error bars of $\bar{S}(h)$ curves indicate the standard deviation. The entropies and their derivatives as functions of h are indicated as solid and dotted lines, respectively. Similar to the cases of histogram estimation, in every case, the vertical axis on the left represents $\bar{S}(h)$, and the right represents the derivative. The mean and the standard deviation are evaluated with 50 instances. Again, the subscript ‘dm’ in the figure indicates ‘derivative’s minimum’.

Table 2. Results derived from kernel estimation. All are parallel to those of histogram estimation. For details see Table 1.

N	1D normal			1D power-law			3D normal		
	h_{dm}	\bar{S}_{dm}	$\sigma(\bar{S}_{dm})$	h_{dm}	\bar{S}_{dm}	$\sigma(\bar{S}_{dm})$	h_{dm}	\bar{S}_{dm}	$\sigma(\bar{S}_{dm})$
10^3	1.846×10^{-1}	1.410	2.128×10^{-2}	4.213×10^{-2}	0.2722	1.040×10^{-2}	1.539×10^{-1}	4.259	3.562×10^{-2}
10^4	8.090×10^{-2}	1.417	6.634×10^{-3}	1.693×10^{-2}	0.2781	3.273×10^{-3}	6.741×10^{-2}	4.255	1.122×10^{-2}
10^5	3.531×10^{-2}	1.418	2.131×10^{-3}	6.804×10^{-3}	0.2796	4.976×10^{-4}	3.531×10^{-2}	4.257	3.990×10^{-3}
10^6	1.855×10^{-2}	1.419	8.126×10^{-4}	3.281×10^{-3}	0.2812	2.454×10^{-5}	1.546×10^{-2}	4.256	1.216×10^{-3}
10^7	8.128×10^{-3}	1.419	2.040×10^{-4}	1.319×10^{-3}	0.2805	1.327×10^{-5}	5.644×10^{-3}	4.257	3.844×10^{-4}
10^8	4.274×10^{-3}	1.419	8.082×10^{-5}	7.631×10^{-4}	0.2804	5.985×10^{-7}	2.473×10^{-3}	4.257	1.240×10^{-4}
theoretic	–	1.419	–	–	0.2804	–	–	4.257	–

in which f' is the first derivative of f , and the functional $R[g]$ is defined for the roughness of g as

$$R(g) = \int_{-\infty}^{+\infty} g(x)^2 dx.$$

Another one is the optimal bandwidth for kernel estimation (Silverman 1986; Jones et al. 1996):

$$h_{AMISE} = \left[\frac{R(K)}{R(f'')(\int x^2 K(x) dx)^2} \right]^{1/5} N^{-1/5}. \quad (11)$$

Note that h_{AMISE} scales with the sample size as $N^{-1/5}$, while Δv^* scales as $N^{-1/3}$.

The kernel estimation is believed to be superior to the histogram method, and indeed, we notice that $\bar{S}(h)$ as well as $d\bar{S}/dh$ are much smoother than their counterparts of histogram estimation. So we just concentrate on the kernel estimation below.

Figure 5 shows the relations of h_{dm} with the sample size N . We see that in all the three cases, differences between h_{dm} and h_{AMISE} are significant, and h_{dm} well scales as $N^{-1/3}$, in contrast to $h_{AMISE} \propto N^{-1/5}$. It is interesting to note that this $N^{-1/3}$ -scaling is similar to that of Scott’s formula of equation (10) for optimal bin width of histogram estimation.

Entropies evaluated at h_{dm} and h_{AMISE} of the three cases are shown in Figure 6. It can be seen that $\bar{S}(h_{dm})$ is much closer to entropy’s true value S_{th} than $\bar{S}(h_{AMISE})$, but the difference between the two vanishes asymptotically with increasing sample size. Nonetheless, as far as the statistical computation of entropy is concerned, h_{AMISE} , selected by minimizing AMISE, is less than the optimal bandwidth h_{dm} .

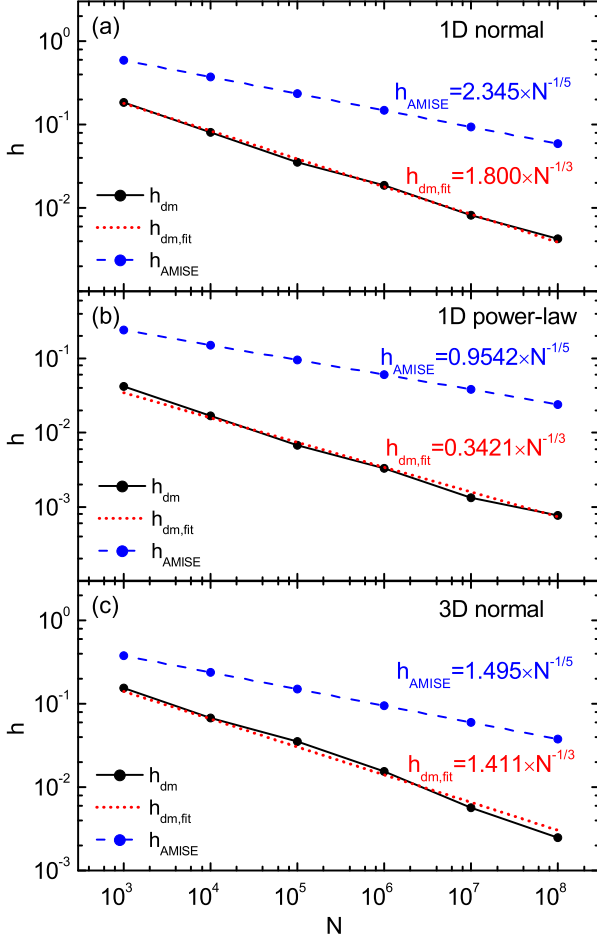


Figure 5. Relation of the bandwidth h and sample size N for the case of kernel estimation. The three panels correspond to the three experimental PDFs of equations (4), (5) and (6). The bandwidth h_{AMISE} that is derived by minimizing AMISE is also shown for comparison.

3.4 The first derivative of entropy as bandwidth selector

From previous results, we have seen that the first derivative of $S(\Delta v)$ or $S(h)$ can be used as a selector for the optimal bin width or bandwidth. We just concentrate on the kernel method here, and present some analytical results. With the estimated PDF \hat{F}_h , the first derivative of the entropy is

$$\begin{aligned} \frac{dS(h)}{dh} &= -\frac{d}{dh} \int \hat{F}_h \ln \hat{F}_h dv \\ &= -\int \left(\frac{\partial \hat{F}_h}{\partial h} \ln \hat{F}_h + \frac{\partial \hat{F}_h}{\partial h} \right) dv \\ &= -\int \frac{\partial \hat{F}_h}{\partial h} \ln \hat{F}_h dv, \end{aligned} \quad (12)$$

in which we use the normalization $\int \hat{F}_h dv = 1$, and the fact that the partial derivative w.r.t. h can be taken out from the integral.

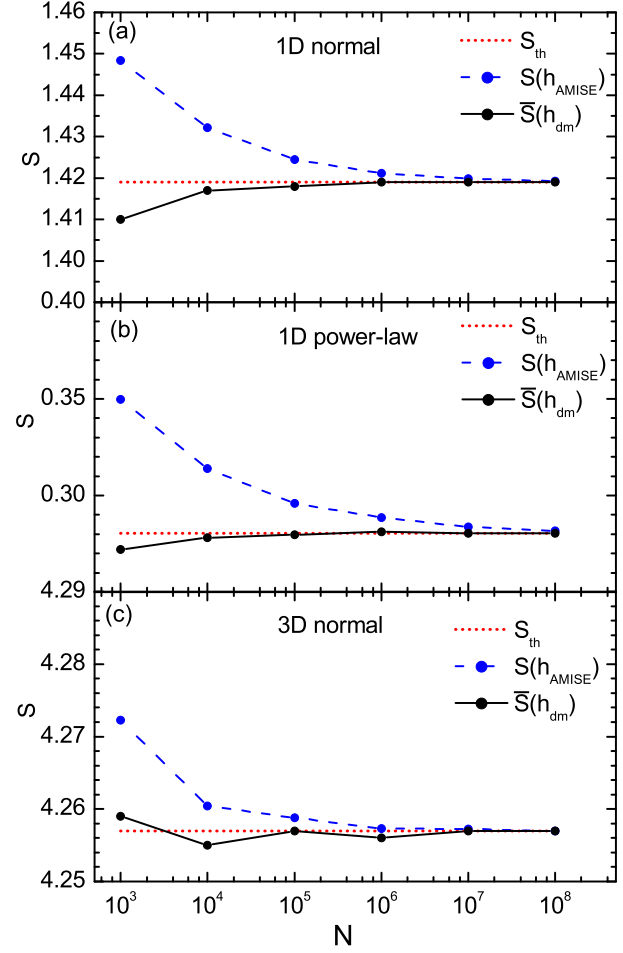


Figure 6. Relation of entropy S and sample size N for the case of kernel estimation. The three panels correspond to the three experimental PDFs of equations (4), (5) and (6). Entropies of h_{AMISE} are also shown for comparison.

The second derivative of $S(h)$ is

$$\begin{aligned} \frac{d^2 S(h)}{dh^2} &= -\int \left[\frac{\partial^2 \hat{F}_h}{\partial h^2} \ln \hat{F}_h + \frac{1}{\hat{F}_h} \left(\frac{\partial \hat{F}_h}{\partial h} \right)^2 \right] dv \\ &= -\int \left(\frac{\partial^2 \hat{F}_h}{\partial h^2} \ln \hat{F}_h - \hat{F}_h \frac{\partial^2 \ln \hat{F}_h}{\partial h^2} + \frac{\partial^2 \hat{F}_h}{\partial h^2} \right) dv \\ &= -\int \frac{\partial^2 \hat{F}_h}{\partial h^2} \ln \hat{F}_h dv + \int \hat{F}_h \frac{\partial^2 \ln \hat{F}_h}{\partial h^2} dv. \end{aligned} \quad (13)$$

In deriving the last line of the above relation, we again use the normalization $\int \hat{F}_h dv = 1$. Hence, the minimum of the first derivative of $S(h)$ should be picked out by $d^2 S/dh^2 = 0$, and from the above equation, we have

$$\int \frac{\partial^2 \hat{F}_h}{\partial h^2} \ln \hat{F}_h dv = \int \hat{F}_h \frac{\partial^2 \ln \hat{F}_h}{\partial h^2} dv. \quad (14)$$

We can make use of this relation to pick out the optimal bandwidth h_{dm} .

Note that both Δv^* of equation (10) and h_{AMISE} of equation (11) depend on the unknown true PDF f , which is usually difficult or even impossible to acquire. On the contrary, the selector of optimal bandwidth based on the first derivative of entropy is

purely data-based, and hence, our approach is much superior to the existing methods.

However, we do not provide a proof on the existence of the minimum of the first derivative of entropy, and do not explain why such a minimum can help pick out the optimal bandwidth, either. These issues are surely of great importance and deserve further investigations.

4 SUMMARY AND DISCUSSIONS

Entropy is a very important concept, and in statistical mechanics, it is computed with the probability distribution function of the system under consideration. In our statistical-mechanical investigations of self-gravitating systems, however, we have to do statistical computation of entropy directly from statistical samples, without knowing the underlying analytic PDF. Thus, the evaluation of entropy is actually related to the estimation of the PDF from statistical samples in data-form.

Usually, there are two approaches to estimate a PDF from a statistical sample. The first density estimation method is histogram. Another way is kernel estimation, which is considered to be superior to the histogram. We use both the methods to evaluate the entropy, and we find that the entropy thus computed depends on the bin width of the histogram, or bandwidth of kernel method. Concretely, the entropy is a monotonic increasing function of the bin width or bandwidth. We attribute this monotonicity to the PDF coarse-graining.

Thus, it is a difficulty on how to select an optimal bin width/bandwidth for computing the entropy. Fortunately, we notice that there may exist a minimum of the first derivatives of entropy for both histogram and kernel estimation, and this minimum may correspond to the optimal bin width and bandwidth.

We perform a large amount of numerical experiments to verify this finding. First, we select three analytical PDFs, one-dimensional standard normal, one-dimensional power-law, and three-dimensional standard normal distribution, and with Monte Carlo technique, we draw N random data from these analytical PDFs, respectively. With these statistical samples, we construct the estimator of the true PDFs of both histogram and kernel estimation. Secondly, we compute the entropy with the estimated PDFs, so in this way, we derive the curves of $S(\Delta v)$ or $S(h)$, in which Δv or h are the bin width of histogram or bandwidth of kernel, respectively. Meanwhile, the entropy can be exactly evaluated with these analytical PDFs. These exact results can be used to calibrate our empirical results, and to help select the optimal bin width or bandwidth.

We do the same experiments for the three PDFs with the sample size ranging from 10^3 to 10^8 . In all cases, whatever using histogram or kernel estimation, we find that:

- The first derivative of entropy indeed has a minimum around the cross-point of the entropy curve $S(\Delta v)$ or $S(h)$ and the theoretical straight line S_{th} .
- The minimum of the derivative goes to zero with increasing sample size.
- Δv_{dm} or h_{dm} , at which the derivative takes its minimum, asymptotically approaches the abscissa of the above-mentioned cross-point with increasing sample size, such that the entropy at Δv_{dm} or h_{dm} asymptotically approaches the theoretical value S_{th} .
- h_{dm} scales with the sample size as $N^{-1/3}$, in contrast to h_{AMISE} , the bandwidth selected by minimizing AMISE, whose scaling is $\propto N^{-1/5}$.

- The entropy evaluated at h_{dm} is much closer to the true value S_{th} than at h_{AMISE} , but the difference between the two vanishes asymptotically with increasing sample size.

Hence, we see that the minimum of the first derivative of $S(\Delta v)$ or $S(h)$ can be used as a selector for the optimal bin-width or bandwidth of density estimation, and h_{AMISE} is less the optimal bandwidth than h_{dm} for computing entropy.

Note that both Scott's optimal bin width Δv^* and h_{AMISE} depend on the unknown underlying PDF of the system, which is usually difficult or even impossible to acquire. On the contrary, the estimator of optimal bandwidth selected from the minimum of the first derivative of entropy is purely data-based, and hence, our method is clearly superior to the existing methods.

We emphasize that our results are by no means restricted to one-dimensional, but can also be extended to multivariate cases. Finally, we acknowledge that we do not provide a robust mathematical proof of the existence of the minimum of the first derivative of entropy, nor theoretically explain why such a minimum can help pick out the optimal bandwidth. These issues are surely of great importance and deserve further investigations. We leave these issues with those specialists who are interested in them.

ACKNOWLEDGEMENTS

We thank the referee very much for many constructive suggestions and comments, especially for the reminding of the techniques for estimating information-theoretic quantities developed by Wolpert & Wolf (1995) and Wolpert & Dedeo (2013). This work is supported by the National Basic Research Program of China (no: 2010CB832805) and by the National Science Foundation of China (no. 11273013), and also supported by the Open Project Program of State Key Laboratory of Theoretical Physics, Institute of Theoretical Physics, Chinese Academy of Sciences, China (no. Y4KF121CJ1).

REFERENCES

- Campa A., Dauxois T., Ruffo S., 2009, Phys. Rep., 480, 57
 Epanechnikov V. K., 1969, Theory Probab. Appl., 14, 153
 Gentle J. E., 2009, Computational Statistics. Springer Science+Business Media, New York
 He P., Kang D. B., 2010, MNRAS, 406, 2678
 He P., Kang D. B., 2011, MNRAS, 414, L21
 He P., 2012, MNRAS, 419, 1667
 He P., 2012, MNRAS, 421, 2088
 Helmi A., White S. D. M., 1999, MNRAS, 307, 495
 Huang K., 1987, Statistical Mechanics. Wiley, New York
 Jones M. C., Marron J. S., Sheather S. J., 1996, J. Am. Stat. Assoc., 91, 401
 Kang D. B., He P., 2011, A&A, 526, A147
 Knuth K. H., 2013, preprint (arXiv:physics/0605197v2)
 Landau L. D., Lifshitz E. M., 1996, Statistical Physics, 3rd Revised edn. Butterworth-Heinemann, London
 Lynden-Bell D., 1967, MNRAS, 136, 101
 Parzen E., 1962, Ann. Math. Stat., 33, 1065
 Rosenblatt M., 1956, Ann. Math. Stat., 27, 832
 Scott D. W., 1979, Biometrika, 66, 605
 Scott D. W., 1992, Multivariate Density Estimation: Theory, Practice, and Visualization, Wiley, New York

- Scott D. W., 2004, Multivariate Density Estimation and Visualization, Papers/Humboldt-Universität Berlin, Center for Applied Statistics and Economics (CASE), No. 2004, 16
- Shannon C. E., 1948, Bell Syst. Tech. J. 27, 379.
- Shunsuke I., 1993, Information theory for continuous systems, World Scientific, Singapore
- Silverman B. W., 1986, Density Estimation for Statistics and Data Analysis, Chapman and Hall, London
- Sturges H. A., 1926, J. Am. Stat. Assoc., 21, 65
- Wand M. P., 1997, Am. Stat., 51, 59
- Wolpert D. H., Wolf D. R., 1995, Phys. Rev. E, 52, 6841
- Wolpert D. H., DeDeo S., 2013, Entropy, 15, 4668